Journal of Molecular Catalysis A: Chemical 346 (2011) 111–116

Contents lists available at ScienceDirect

Journal of Molecular Catalysis A: Chemical

journal homepage: www.elsevier.com/locate/molcata

Photocatalytic degradation of methylene blue in water using $CoFe_2O_4$–Cr_2O_3–SiO_2 fluorescent magnetic nanocomposite

Kula Kamal Senapati [a], Chandan Borgohain [a,b], Kanak C. Sarma [b], Prodeep Phukan [a,*]

[a] Department of Chemistry, Gauhati University, Guwahati 781014, Assam, India
[b] USIC, Gauhati University, Guwahati 781014, Assam, India

ARTICLE INFO

Article history:
Received 28 May 2011
Received in revised form 1 July 2011
Accepted 3 July 2011
Available online 7 July 2011

Keywords:
Magnetic nanocomposite
Photocatalyst
Organic pollutant
Co-precipitation
Wastewater

ABSTRACT

A $CoFe_2O_4$–Cr_2O_3–SiO_2 fluorescent magnetic nanocomposite (FMNC) has been synthesized by a combined sonochemical co-precipitation method. Remarkable feature of the FMNC is its high band gap energy (3–4 eV). Photocatalytic activity of the FMNC has been examined for degradation of methylene blue in aqueous solution under UV irradiation (12 mW Hg lamp, major wavelength 400 nm). The catalyst could be separated from aqueous media by applying external magnetic field and hence could be reused without any significant loss of its activity.

1. Introduction:

Organic dyes are the major constituent of pollutants in wastewater released from textile and other industries. Discharge of those colored wastewaters in the ecosystems causes serious environmental problems like aesthetic pollution, eutrophication and can originate dangerous byproducts through oxidation, hydrolysis, or other chemical reactions in the wastewater phase [1–4]. A variety of methods such as adsorption [5], biodegradation [6] and chemical methods [7] were presently available for wastewater treatment. The use of homogeneous catalyst for wastewater treatment suffers the disadvantage of recovery and reusability and may result in secondary pollution by releasing metal ion in to water [8–12]. Hence, many catalyst supports such as beaded glass, silica gel, activated carbon and recently carbon nano tubes were used for immobilization of homogeneous catalyst. In this regard, heterogeneous photocatalytic methods have been appeared as promising destructive technology leading to total mineralization of most organic pollutants [13–17]. Generally, the degradation of organic pollutants in water is conducted with semiconductors such as TiO_2, CdS and ZnO under UV-irradiation [18]. However, one serious drawback of suspended photocatalyst lie in that they get agglomerated in aqueous solution, hinder the penetration of light illumination and hence lower photocatalytic efficiency.

The use of magnetic nanoparticles as support or catalysts has attracted considerable interest in recent years, because they offer significant advantages such as high surface area-to-volume ratios and easy magnetic separation [19–21]. Cobalt ferrite ($CoFe_2O_4$) magnetic nanoparticles are considered as a better support due to their high thermal and chemical stability, structural stability, tunable size and magnetic properties [22]. We have recently developed a new $CoFe_2O_4$–Cr_2O_3–SiO_2 nanocomposite of 30 ± 5 nm sizes having photoluminescence properties, which was further, utilized for bio-imaging human cervical cancer cells [23]. We observed that the $CoFe_2O_4$–Cr_2O_3–SiO_2 nanocomposite has remarkably high band gap energy. This prompted us to use it for photocatalytic degradation of an organic pollutant. While no investigation of photocatalytic behavior on such nanocomposites have been reported so far, development of such catalyst may provide us a powerful approach for waste water treatment with an additional advantage of easy magnetic recovery and reusability. In this study we are reporting the photo catalytic degradation of a typical organic dye, methylene blue (MB), as a representative case using the new magnetic nanocomposite.

2. Experimental

2.1. Synthesis of $CoFe_2O_4$–Cr_2O_3–SiO_2 FMNC

Synthesis of $CoFe_2O_4$–Cr_2O_3–SiO_2 FMNCs was achieved by a combined sonochemical and co-precipitation technique [23]. Initially uncapped $CoFe_2O_4$ was synthesized which was then

* Corresponding author. Tel.: +91 361 2570535; fax: +91 361 2700311.
E-mail address: pphukan@yahoo.com (P. Phukan).

1381-1169/$ – see front matter © 2011 Elsevier B.V. All rights reserved.
doi:10.1016/j.molcata.2011.07.001

coated with Cr_2O_3. The final step involves the coating of the $CoFe_2O_4$–Cr_2O_3 nanoparticles with tetraethylorthosilicate followed by annealing at high temperature. The procedure is described below.

2.1.1. Synthesis of $CoFe_2O_4$ NP

A mixture of two aqueous solutions of $FeCl_3$ (1.5 g, 9.3 mmol, 50 mL) and $CoCl_2{\cdot}6H_2O$ (1 g, 4.2 mmol, 50 mL) in a conical flask was placed in an ultrasonic bath. To this mixture, an aqueous KOH solution (3 M, 25 mL) was added dropwise under argon atmosphere with continuous ultrasonic irradiation (frequency 40 kHz and power of 40 kW). Prior to mixing, all these three solutions were made oxygen-free by sonicating for 30 min. The temperature of the sonicator bath was raised up to 60 °C and the mixture was further sonicated for 30 min in air atmosphere. The reaction mixture was centrifuged (14,000 rpm) at ambient temperature for 15 min. The mixture was further subjected to successive sonication (30 min) and centrifugation (15 min) for five times. The black precipitate was then separated, washed with sufficient amount of distilled water, ethanol and kept overnight in an incubator at 60 °C for ageing. The precipitate was further dried in oven at 100 °C for one hour and subsequently kept under high vacuum (10^{-2} bar) for one hour. Finally, the black particles were taken in 50 mL of dry ethanol and subjected to successive sonicaiton (30 min) and centrifugation (15 min) repeatedly till a brown colored solution appears. The precipitate was separated by centrifugation, dried and used for further modification.

2.1.2. Synthesis of $CoFe_2O_4$–Cr_2O_3 NC

A dispersion of the above $CoFe_2O_4$ nanoparticles (0.4 mmol) in deionised water was taken with appropriate molar ratios of $Cr(OAc)_3{\cdot}H_2O$ (0.01 mmol) in a round bottom flask. An aqueous solution of NaOH (3 M) was added to the mixture with constant ultrasonic irradiation (frequency 40 kHz at 40 kW). Prior to mixing, all these four solutions were degassed by sonication for 30 min. The reaction mixture was further sonicated for 30 min at 60 °C in air. The brown precipitate formed was separated by centrifugation (10,000 rpm) and washed with copious amount of distilled water followed by ethanol and kept overnight in an incubator at 60 °C for ageing. The precipitate was further dried in oven at 100 °C for one hour and subsequently kept under high vacuum (10^{-2} bar) for one hour. Finally, the particles were taken in 50 mL of dry ethanol and subjected to successive sonication (30 min) and centrifugation (15 min) repeatedly till a brown colored solution appears. The precipitate was separated, dried and held at 1000 °C in a muffle furnace for 10 h to obtain a fine black powder. Energy dispersive X-ray spectroscopy (EDX) analysis at this point showed excellent agreement between expected and observed values of the constituent elements and therefore confirms the formation of $CoFe_2O_4$–Cr_2O_3.

2.1.3. Surface modification of $CoFe_2O_4$–Cr_2O_3 nanoparticle by SiO_2

The as prepared $CoFe_2O_4$–Cr_2O_3 nanoparticle was coated with silica by treating with tetraethyl orthosilicate (TEOS) [24]. TEOS (0.5 mL) was added to a dispersion of $CoFe_2O_4$–Cr_2O_3 nanoparticles (0.2 g) in to a mixture of ethanol (20 mL), water (9 mL) and ammonia (25%, 0.5 mL) under ultrasonication. After 3 h, the precipitate was isolated by centrifugation and washed with ethanol and water several times and dried at 80 °C under vacuum for 2 h.

2.2. Characterization

Structural characterization was performed by means of X-ray diffractometer (Bruker AXD D8) with Cu Kα radiation (λ = 1.54178 Å). Morphology of the FMNCs was investigated by a 200 kV transmission electron microscope (TEM) (JEOL JEM2100, Japan). Quantitative elemental analysis was carried out with an energy dispersive X-ray spectrometer (EDX) (Oxford, UK) mounted on the TEM. The photocatalytic activity of $CoFe_2O_4$–Cr_2O_3 nanocomposite was evaluated by UV–vis spectroscopy (Cary 50 Bio, Varian). The magnetic properties of the as prepared $CoFe_2O_4$, $CoFe_2O_4$–Cr_2O_3 and $CoFe_2O_4$–Cr_2O_3–SiO_2 nanoparticles were investigated by vibrating sample magnetometer (Lakeshore 7410). The fluorescent properties of the nanoparticles were measured in the time-resolved steady state photoluminescence spectrometer (Eddinburg FSP920).

2.3. Photocatalytic degradation

The photocatalytic degradation of methylene blue using $CoFe_2O_4$–Cr_2O_3–SiO_2 FMNC was carried out as follows.

A dispersion of FMNCs (0.02 g) was made in 1×10^{-6} M aqueous solution of methylene blue (50 mL) by ultrasonication for 10 min and the dispersion was kept in dark with stirring for 30 min to reach the absorption–desorption equilibrium. Then, the dispersion was placed in a 200 mL cylindrical quartz tube with stirring facility and kept under UV irradiation (12 mW, major wavelength 400 nm). The reaction was monitored by using UV–vis spectrophotometer in the wavelength range of 200–800 nm. Finally, photocatalytic degradation percentage of MB was calculated using Eq. (1)

$$\text{Degradation}\,(\%) = \left(\frac{A_0 - A}{A_0}\right) \times 100 \quad (1)$$

where A_0 and A are the UV–vis absorption of original and sampled solutions, respectively.

3. Results and discussion

3.1. Synthesis of $CoFe_2O_4$–Cr_2O_3–SiO_2 FMNC

The $CoFe_2O_4$–Cr_2O_3–SiO_2 nanocomposite was prepared by a three-step process [23]. Initially, cobalt ferrite nanoparticles were synthesized by means of a combined sonochemical and co-precipitation technique in aqueous medium without any capping agent. The synthesis was carried out in an alkaline pH under repetitive ultrasonic irradiation. In the next step, the as synthesized $CoFe_2O_4$ nanoparticles were coated with a layer of Cr_2O_3 on the surface by treating a premixed aqueous dispersion of $CoFe_2O_4$ nanoparticles and $Cr(OAc)_3{\cdot}H_2O$ with NaOH (3 M) under ultrasonic irradiation. The $CoFe_2O_4$–Cr_2O_3 nanocomposite was then heated at 1000 °C and finally surface coated with SiO_2 using tetraethyl orthosilicate to get the $CoFe_2O_4$–Cr_2O_3–SiO_2 nanocomposite.

3.2. Characterization of $CoFe_2O_4$–Cr_2O_3–SiO_2 FMNC

3.2.1. Structural analysis

The XRD pattern of the $CoFe_2O_4$–Cr_2O_3 (Supporting information) and SiO_2 coated $CoFe_2O_4$–Cr_2O_3–SiO_2 (Fig. 1) nanocomposite shows the characteristics peak for the pure magnetic core of spinel $CoFe_2O_4$ (JCPDS – International Center diffraction data, PDF card 3-864 and 22-1086) along with Cr_2O_3 phases (JCPDS – International Center diffraction data, PDF cards 06-0504) and SiO_2 layer. The IR spectra (Supporting information) of the nanocomposite clearly indicated the formation of $CoFe_2O_4$–Cr_2O_3 nanocomposite. In particular, the peak appearing at 575 cm^{-1} corresponds to Cr–O bond of the nanocomposite.

3.2.2. TEM and EDX analysis

The structural composition and crystallinity of the cobalt ferrite nanoparticles was further examined using TEM and EDX measurement and are presented in Figs. 2 and 3 respectively by depositing $CoFe_2O_4$–Cr_2O_3–SiO_2 nanocomposite on a carbon-coated copper

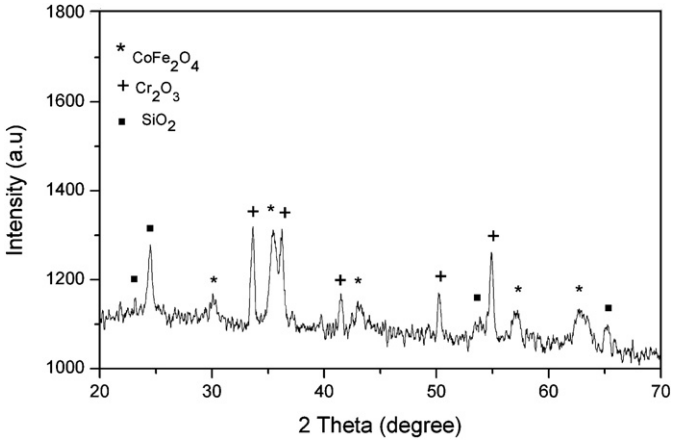

Fig. 1. XRD pattern of $CoFe_2O_4$–Cr_2O_3–SiO_2 NC.

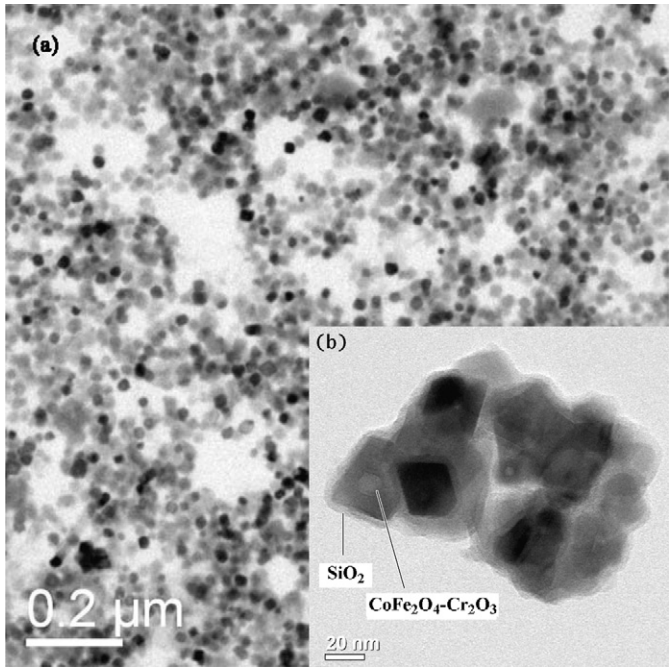

Fig. 2. TEM image of $CoFe_2O_4$–Cr_2O_3–SiO_2 FMNC at magnification of (a) 20× k and (b) 50× k.

grid. The TEM image shows that the $CoFe_2O_4$–Cr_2O_3 nanocomposite is covered by a thin coating layer of SiO_2. The average size of the nanocomposite from the TEM analysis was found to be 30 ± 5 nm. The TEM images of the primary $CoFe_2O_4$ nanoparticles

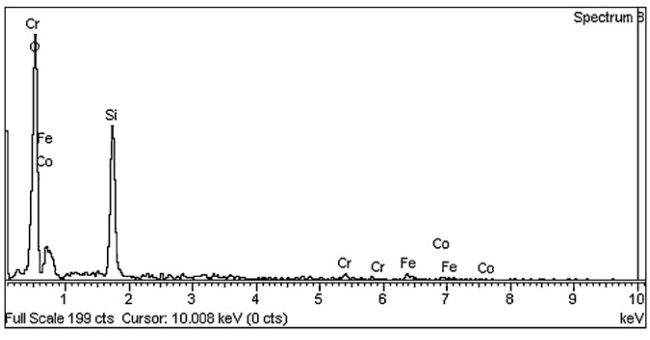

Fig. 3. EDX spectra of $CoFe_2O_4$–Cr_2O_3–SiO_2 NC.

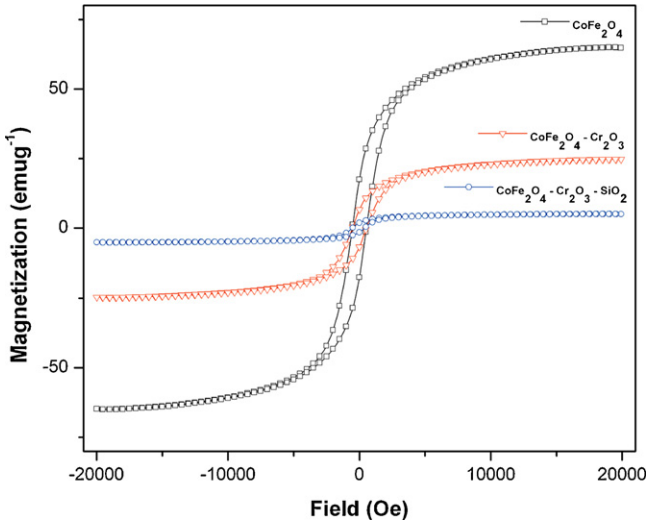

Fig. 4. M–H loops of $CoFe_2O_4$, $CoFe_2O_4$–Cr_2O_3 and $CoFe_2O_4$–Cr_2O_3–SiO_2 nanocomposite.

and $CoFe_2O_4$–Cr_2O_3 nanocomposites are provided in Supporting information where the Cr_2O_3 nanoparticles are clearly seen over the $CoFe_2O_4$ nanocrystals.

The EDX analysis in TEM measurement gave the elemental distribution (atomic percent) in the FMNC as Co = 5.9%, Fe = 11.6%, Cr = 11%, O = 54%, Si = 17.5%. Thus the Fe/Co ratio in the nanocomposite by EDX was found to be 1.9 which is close to the atomic ratio in the $CoFe_2O_4$ along with contributions from Cr, O and Si without any impurity.

3.2.3. Magnetic properties

Magnetic measurements for the $CoFe_2O_4$ magnetic core as well as the nanocomposites were carried out to examine the effect of incorporation of Cr_2O_3 and SiO_2 on the magnetic core. Incorporation of antiferromagnetic Cr_2O_3 and SiO_2 in the magnetic core changes the magnetic property of the core material. The magnetization–hysteresis (M–H) loop was taken at room temperature with a maximum applied field of ±2 T and shown in Fig. 4. From the hysteresis loop, the saturation magnetization (Ms), coercivity (Hc) and retentivity (Mr) were evaluated. The Ms values were found to be 64.97, 24.74, and 5.10 emu g^{-1} for $CoFe_2O_4$, $CoFe_2O_4$–Cr_2O_3 and $CoFe_2O_4$–Cr_2O_3–SiO_2 respectively.

Similarly, the Hc values of 539, 529 and 482 Oe and the Mr values of 17.49, 6.62, 1.79 emu g^{-1} were obtained for the $CoFe_2O_4$, $CoFe_2O_4$–Cr_2O_3 and $CoFe_2O_4$–Cr_2O_3–SiO_2 respectively. It was observed that incorporation of Cr_2O_3 and SiO_2 in the Co–Fe–O matrix had very little effect on the coercivity (Hc); however the magnetization (Ms) and the retentivity (Mr) decreased rapidly.

Thus by controlling the quantity of Cr_2O_3 and SiO_2 in the $CoFe_2O_4$ magnetic core, the properties of the nanocomposite could be tailored to suite different catalytic applications.

3.2.4. Spectral analysis

Fig. 5(a) and (b) shows the UV–vis absorption and fluorescence emission (excitation at 372 nm) spectra of aqueous dispersion of the $CoFe_2O_4$–Cr_2O_3–SiO_2 nanocomposite.

A sharp peak at 200 nm of the UV–vis spectrum indicates that the colloids are well dispersed. The spectrum shows two absorption bands at around 270 nm and 370 nm which are due to the presence of Cr_2O_3 in the sample. The bandgap energies corresponding to these absorption bands were determined to be of 3.0 eV and 4.02 eV respectively following Tauc relation [25] (Fig. 6). In case of as synthesized Cr_2O_3 (Supplementary information), two peaks at

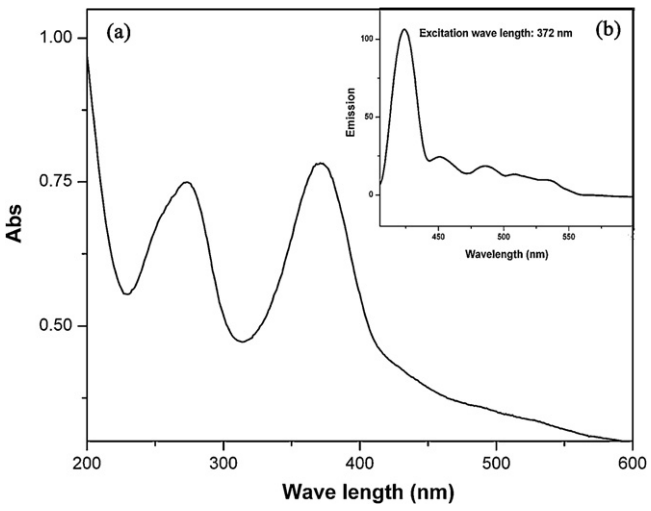

Fig. 5. UV–vis absorption and fluorescence emission (excitation at 372 nm) spectra of $CoFe_2O_4$–Cr_2O_3–SiO_2 NC.

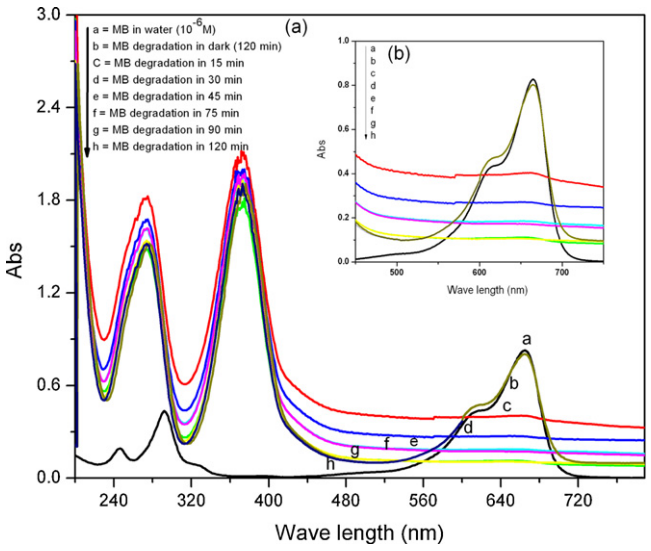

Fig. 7. UV–vis spectra of MB degradation by $CoFe_2O_4$–Cr_2O_3–SiO_2 NC.

274 and 373 nm were observed and a slight blue shift was noticed in $CoFe_2O_4$–Cr_2O_3 (Supplementary information) sample as compared to pure Cr_2O_3. Fig. 5b shows sharp photoluminescence (PL) spectra obtained from $CoFe_2O_4$–Cr_2O_3–SiO_2 nanocomposite in aqueous medium at room temperature. The maximum intensity of emission at 425 nm was obtained when the excitation energy at 372 nm wavelength was used. The observed PL is due to the formation of defect created by deficiency of Cr-ions in Cr_2O_3 in high temperature annealing during preparation of $CoFe_2O_4$–Cr_2O_3 NC [23].

3.3. Photocatalytic activity

3.3.1. Spectral measurement

Since the as-prepared ferromagnetic nanocomposite exhibits photoluminescence property and has high band gap energy, we sought to explore the possibility of use of such material for photodegradation of organic pollutant. Recently, a composite material of TiO_2 semiconductor with $CoFe_2O_4$ as magnetic core has been reported to be a useful photocatalyst for degradation of organic contaminants in water [26]. However, no one has addressed the possibility of a photocatalyst incorporating Cr_2O_3 on the surface of a magnetic core such as Fe_3O_4 or $CoFe_2O_4$ till date. To demonstrate the potential application of the $CoFe_2O_4$–Cr_2O_3–SiO_2 fluorescence

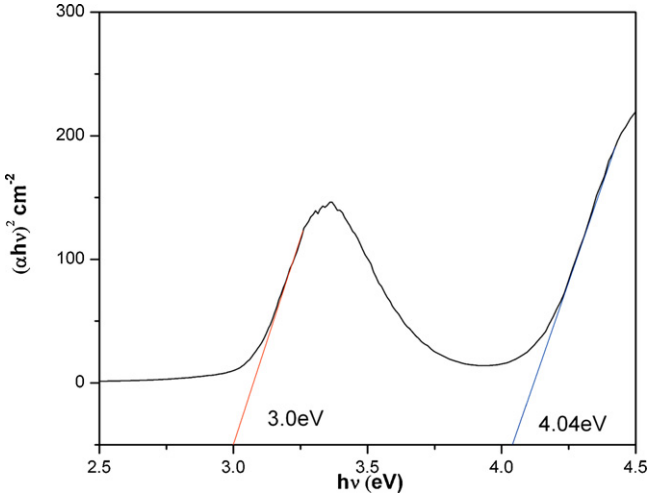

Fig. 6. Bandgap energies of $CoFe_2O_4$–Cr_2O_3–SiO_2 nanocoposite.

magnetic nanocomposite, we examined the photocatalytic activity of the nanocomposite for degradation of methylene blue as a model reaction.

The catalytic performance was tested under UV lamp (12 mW Hg lamp, major wavelength 400 nm) at ambient temperature. Fig. 7 shows the absorption spectra of the aqueous solution of MB exposed to UV light for various time periods. The typical absorption peak at 664 nm gradually diminished with increasing the UV exposure time and almost completely disappeared after 120 min, suggesting the nearly complete degradation of MB by the FMNC. It was observed that the degradation of MB was faster initially (almost 51% in 15 min) and decreased thereafter. A typical run without UV-irradiation by stirring the reaction mixture in dark for 120 min confirms that photo-oxidation does not take place in absence of UV light (spectral line b in Fig. 7). The observed high photocatalytic activity is due to (a) remarkably high band gap energy for the MNCs, as the photocatalytic effect depends on the enhancement in electron-hole (e^-/h^+) separation [27] and (b) small particle size which is associated with high surface area. Secondly, in photocatalytic degradation of organic compounds by semiconductors, a dopant such as Cr_2O_3 ion may act as an electron trap or hole trap which in turn prolong the lifetime of the generated charge carriers, resulting in enhanced photocatalytic activity [26]. It is well known that both $CoFe_2O_4$ and Cr_2O_3 are p-type semiconductors. On thermal treatment, Cr_2O_3 becomes slightly nonstoichiometric, generally known as $Cr_{2-x}O_3$ and the probability of diffusion of Cr into the spinel structure of $CoFe_2O_4$ increases during high temperature annealing process in synthesis. On the other hand, Cr doped $CoFe_2O_4$ is an n-type semiconductor. Therefore at the interface of $CoFe_2O_4$ and Cr_2O_3, a p–n junction is formed which can enhance charge separation of photo-generated e^-/h^+ pairs and consequently improve the photocatalytic efficiency.

For comparison, we have also evaluated the catalytic performance of the $CoFe_2O_4$–Cr_2O_3 (without coating with SiO_2) and the result is shown in Fig. 8. We found that the uncoated $CoFe_2O_4$–Cr_2O_3 composite did not exhibit significant catalytic activity with only 10% decrease in the concentration of MB in 120 min under UV irradiation. The enhanced photocatalytic activity of $CoFe_2O_4$–Cr_2O_3–SiO_2 compared to $CoFe_2O_4$–Cr_2O_3 for MB decomposition is due to the surface coating of SiO_2. Although SiO_2 itself is not catalytically active, we have observed that it enhances the photocatalytic activity of the composite. The SiO_2 forms a porous membrane round the surface of $CoFe_2O_4$–Cr_2O_3

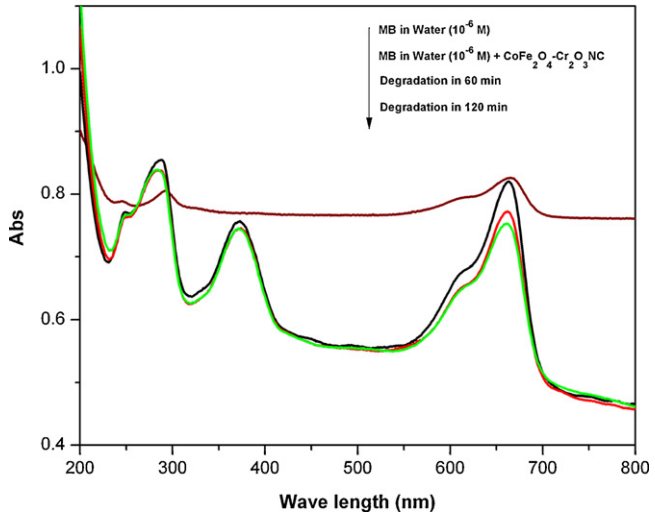

Fig. 8. UV–vis spectra of MB degradation by $CoFe_2O_4$–Cr_2O_3 NC.

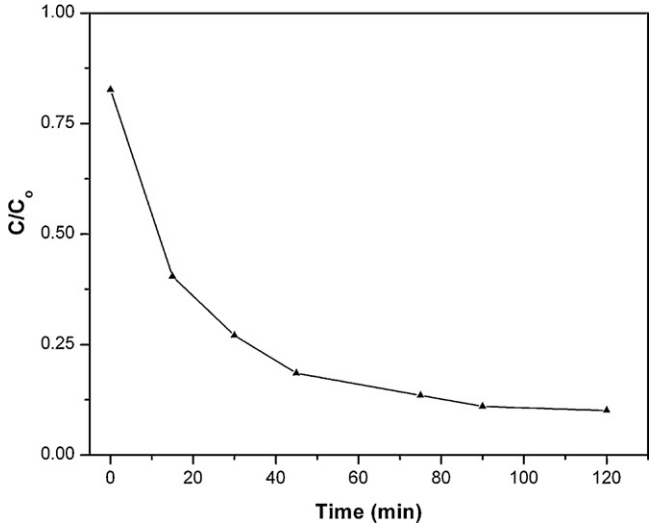

Fig. 9. First-order representation of decomposition of MB by $CoFe_2O_4$–Cr_2O_3–SiO_2 NC vs. time.

nanoparticles, which might serve as an effective polar surface and renders complete dispersibility in water and hence more exposed to UV radiation. On the contrary, the uncoated $CoFe_2O_4$–Cr_2O_3 nanocomposite is weakly dispersed in aqueous medium and gets agglomerated in due course of time and thus accounts for its very low photocatalytic activity. Pure SiO_2 is known to be UV-transparent and hence the outer membrane allows the organic molecules to come into contact with the active layer which finally get degraded in presence of UV radiation. Therefore the coating of SiO_2 was necessary to prevent self-degradation and promote efficient dispersion of nanoparticles in solution and accordingly play a vital role in photocatalytic degradation of methylene blue solution.

The UV absorption spectrum as well as the fluorescence emission spectrum (excitation at 372 nm) of the nano composites did not show any significant changes in position and intensity during photo degradation measurement which shows the stability of the nanoparticles. The magnetic nanocatalyst could be easily separated from the reaction media by applying external magnetic field. It is noteworthy that pure $CoFe_2O_4$ nanoparticles can hardly degrade MB solution, but exhibit good magnetism. Secondly, pure Cr_2O_3 shows very low photocatalytic activity [28] and cannot be recovered from the reaction media by external magnet due to its anti-ferromagnetic behavior. However, a careful combination of these with SiO_2 coating could result in a magnificent $CoFe_2O_4$–Cr_2O_3–SiO_2 nanocomposite photocatalyst with optimal level for magnetic separation.

3.3.2. Kinetics

The kinetics of disappearance of methylene blue is illustrated in Fig. 9.

The results show that the photocatalytic degradation of methylene blue dye can be described by the first order kinetic model which can be expressed as follows:

$$\ln\left(\frac{C_o}{C}\right) = kt \qquad (1')$$

where C_o is the initial MB concentration, and C is the concentration at a certain time, k is reaction rate constant, and t is time. C_o/C can be substituted by A_0/A for the reason that the concentration is basically directly proportional to the absorbance. The plots of the concentration data gave a straight line. The apparent first order linear transforms are given in Fig. 10. The slope yield apparent rate constants of 0.025 min^{-1}. The experimental results were well supported to the reported data for photocatalytic decomposition of MB aqueous solution [29–31].

3.3.3. Recyclability of the photocatalyst

The recyclability of the photocatalyst was further investigated by separating the nanocomposite by external magnet. Results were presented in Fig. 11. The recovered nanocomposite was recycled for three times for photodegradation of fresh methylene blue solution without significant loss of catalytic activity.

Fig. 12 shows the fluorescence emission spectra of the recycled nanocomposite in the reaction medium in three consecutive cycles. From these results it can be concluded that the photocatalytic activity of the recycled nanocomposite had no significant loss after three cycles, which indicates the stability and effectiveness of the catalyst for removal of organic pollutants in water. Moreover, the fluorescence emission spectra of recycled catalyst account for its fluorescence stability during repeated photocatalytic cycles.

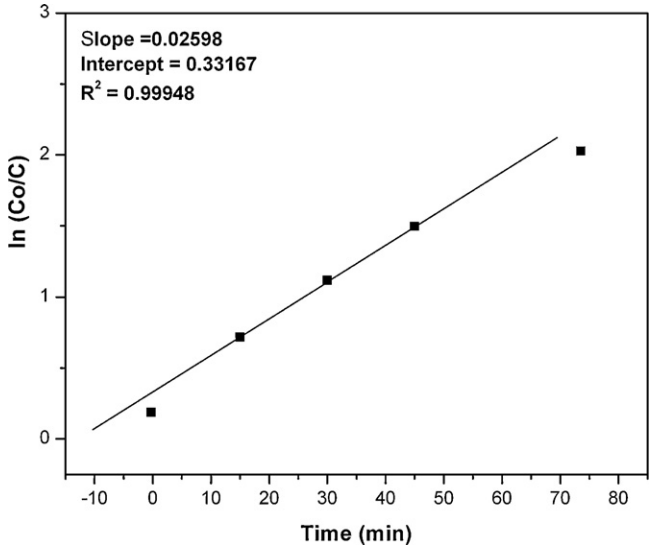

Fig. 10. First-order kinetics for MB photocatalyzed degradation under UV-irradiation.

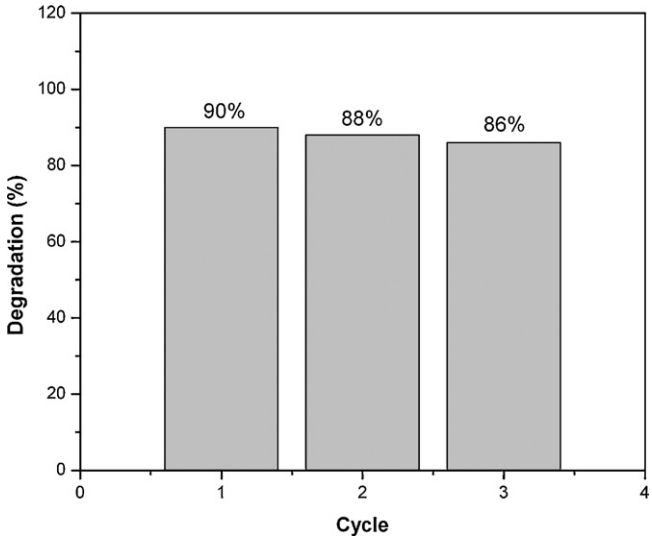

Fig. 11. Photocatalytic degradation of MB in three catalytic cycles.

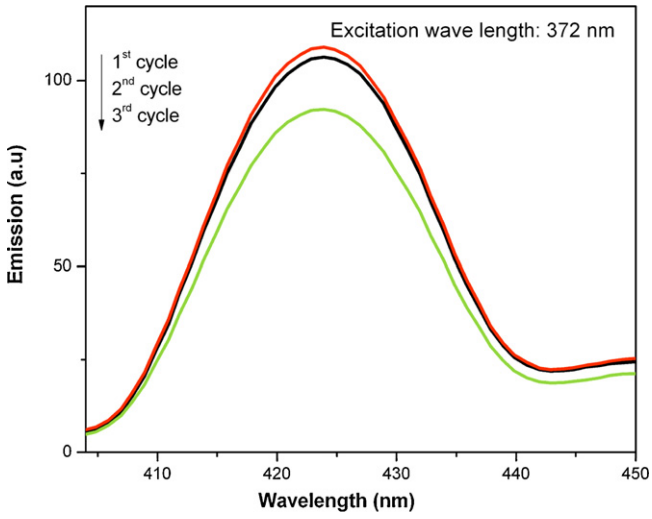

Fig. 12. Fluorescence emission spectra of the reaction mixture in three repeated cycles of photocatalysis.

4. Conclusion

In conclusion, a new type of $CoFe_2O_4$–Cr_2O_3–SiO_2 fluorescence magnetic nanocomposite has been prepared and utilized as photocatalyst for degradation of methylene blue in aqueous solution. The associated magnetic activity of the ferrite core allows easy separation of the photocatalyst after the reaction. The FMNC exhibits high photocatalytic efficiency toward oxidative degradation of organic pollutants such as methyl orange in aqueous solution and could be recycled without appreciable loss of its activity. These results suggest that the FMNC is very suitable for potential applications in organic waste removal from water.

Acknowledgement

Financial support from DST (India) (Grant No. SR/S1/RFPC-07/2006) is gratefully acknowledged. We thank IIT Guwahati for analytical facilities.

Appendix A. Supplementary data

Supplementary data associated with this article can be found, in the online version, at doi:10.1016/j.molcata.2011.07.001.

References

[1] U. Pagga, D. Bruan, Chemosphere 15 (1986) 479.
[2] A.B. Prevot, C. Baiocchi, M.C. Brussino, E. Pramauro, P. Savarino, V. Augugliaro, G. Marci, L. Palmisano, Environ. Sci. Technol. 35 (2001) 971.
[3] B. Neppolian, H.C. Choi, S. Sakthivel, B. Arabindoo, V. Murugesan, Chemosphere 46 (2002) 1173.
[4] M. Saquib, M. Muneer, Dyes Pigments 56 (2003) 37.
[5] P.B. Dejohn, R.A. Hutchins, Text. Chem. Color. 8 (1976) 69.
[6] S.S. Patil, V.M. Shinde, Environ. Sci. Technol. 22 (1988) 1160; A.T. More, A. Vira, S. Fogel, Environ. Sci. Technol. 23 (1989) 403.
[7] Y.M. Slokar, A.M. Le Marechal, Dyes Pigments 37 (1998) 335.
[8] K. Fajerwerg, H. Debellefontaine, Appl. Catal. B 10 (1996) L229.
[9] X. Tao, W.H. Ma, J. Li, Y.P. Huang, J.C. Zhao, J.C. Yu, Chem. Commun. 1 (2003) 80.
[10] J. Fernandez, J. Bandara, A. Lopez, P. Buffat, J. Kiwi, Langmuir 15 (1999) 185.
[11] C. Pulgarin, P. Peringer, P. Albers, J. Kiwi, J. Mol. Catal. A: Chem. 95 (1995) 61.
[12] A.C. Yip, F.L. Lam, X.J. Hu, Chem. Commun. 25 (2005) 3218.
[13] J.C. Crittenden, R.P.S. Suri, D.L. Perram, Water Res. 31 (1997) 411.
[14] J.M. Herrmann, Water treatment by heterogeneous photocatalysis , in: F. Jansen, R.A. van Santen (Eds.), Environmental Catalysis, Catalytic Science Series, vol. 1, Imperial College Press, London, 1999, pp. 171–194 (Chapter 9).
[15] M. Schiavello, Photocatalysis and Environment: Trends and Applications , Kluwer Academic Publishers, Dordrecht, 1988.
[16] N. Serpone, E. Pelizzetti, Photocatalysis, Fundamentals and Applications , Wiley Interscience, New York, 1989.
[17] O. Legrini, E. Oliveros, A.M. Braun, Chem. Rev. 93 (1993) 671.
[18] W.F. Shangguan, Chin. J. Inorg. Chem. 17 (2001) 619.
[19] A.-H. Lu, E.L. Salabas, F. Schüth, Angew. Chem. Int. Ed. 46 (2007) 1222.
[20] Y. Zhu, L.P. Stubbs, F. Ho, R. Liu, C.P. Ship, J.A. Maguire, N.S. Hosmane, ChemCatChem 2 (2010) 365.
[21] K.K. Senapati, C. Borgohain, P. Phukan, J. Mol. Catal. A: Chem. 339 (2011) 24.
[22] M.A.G. Soler, T.F.O. Melo, S.W. da Silva, E.C.D. Lima, A.C.M. Pimenta, V.K. Garg, A.C. Oliviera, P.C. Morais, J. Magn. Magn. Mater. 272 (2004) 2357.
[23] C. Borgohain, K.K. Senapati, D. Mishra, K.C. Sarma, P. Phukan, Nanoscale 2 (2010) 2250.
[24] M. Yu, J. Lin, J. Fang, Chem. Mater. 17 (2005) 1783.
[25] J. Tauc, Amorphous and Liquid Semiconductors , Plenum, New York, 1974.
[26] H.A.J.L. Mourão, A.R. Malagutti, C. Ribeiro, Appl. Catal. A: Gen. 382 (2010) 284.
[27] J. Yu, J. Xiong, B. Cheng, S. Liu, Appl. Catal. B 60 (2005) 211.
[28] Y.S. Jung, K.H. Kim, T.Y. Jang, Y. Tak, S.H. Baeck, Curr. Appl. Phys. 11 (2011) 358.
[29] F. Banat, S. A1-Asheh, M. A1-Rawashdeh, M. Nusair, Desalination 181 (2005) 225.
[30] M.J. Height, S.E. Pratsinis, O. Mekasuwandumrong, P. Praserthdam, Appl. Catal. B: Environ. 63 (2006) 305.
[31] V. Luca, M. Osborne, D. Sizgek, C. Griffith, P.Z. Araujo, Chem. Mater. 18 (2006) 6132.